**Converging on the orb: denser taxon sampling elucidates spider phylogeny and new analytical methods support repeated evolution of the orb web**

Robert J. Kallal[1, 2*], Siddharth S. Kulkarni[1,2], Dimitar Dimitrov[3], Ligia R. Benavides[4], Miquel A. Arnedo[5], Gonzalo Giribet[4], Gustavo Hormiga[1*]

[1]Department of Biological Sciences, The George Washington University, 2029 G St. NW, Washington, D.C. 20052, USA

[2]Department of Entomology, National Museum of Natural History, 10th & Constitution Ave. NW, Washington, DC, 20560, USA

[3]Department of Natural History, University Museum of Bergen, University of Bergen, P.O. Box 7800, 5020 Bergen, Norway

[4]Museum of Comparative Zoology, Department of Organismic and Evolutionary Biology, Harvard University, 26 Oxford Street, Cambridge, MA 02138, USA

[5]Department of Evolutionary Biology, Ecology and Environmental Sciences, & Biodiversity Research Institute (IRBio) Universitat de Barcelona, Avinguda Diagonal 643, Barcelona, Spain

*Correspondence to be sent to: Department of Biological Sciences, The George Washington University, 2029 G St. NW, Washington, D.C. 20052, USA; E-mail: hormiga@gwu.edu and/or Department of Entomology, National Museum of Natural History, 10th & Constitution Ave. NW, Washington, DC, 20560, USA; E-mail: kallalr@si.edu

**Abstract**

High throughput sequencing and phylogenomic analyses focusing on relationships among spiders have both reinforced and upturned long-standing hypotheses. Similarly, the evolution of spider webs – perhaps their most emblematic attribute – is being understood in new ways. With a matrix including 272 spider species and close arachnid relatives, we analyze and evaluate the relationships among these lineages using a variety of orthology assessment methods, occupancy thresholds, tree inference methods, and support metrics. Our analyses include families not previously sampled in transcriptomic analyses, such as Symphytognathidae, the only araneoid family absent in prior such works. We find support for the major established spider lineages, including Mygalomorphae, Araneomorphae, Synspermiata, Palpimanoidea, Araneoidea, and the RTA Clade, as well as the UDOH Grade. Resulting trees are evaluated using bootstrapping, SH-aLRT, local posterior probabilities, and concordance factors. Using structured Markov models to assess the evolution of spider webs while accounting for hierarchically nested traits, we find multiple convergent occurrences of the orb web across the spider tree of life. Overall, we provide the most comprehensive spider tree of life to date using transcriptomic data and use new methods to explore controversial issues of web evolution, including the origins and multiple losses of the orb web.

Keywords: Araneae, concordance factors, maximum likelihood, penalized likelihood, structured Markov models

Table of contents

Introduction

Spiders (Araneae) are omnipresent predators and comprise one of the most diverse animal orders outside Hexapoda (Zhang, 2011). Over the course of several hundred million years, spiders have evolved into myriad shapes and sizes, filling niches in virtually all terrestrial (and some aquatic) habitats, except in Antarctica. Currently, over 48,000 species are described among 120 families (World Spider Catalog, 2020), with three families described in 2019 alone (Hedin et al., 2019; Ramírez et al., 2019). One of the most iconic traits of spiders is the production of silk, along with its many uses. A handful of gland types secrete silk used for producing egg sacs, bonding to substrates, wrapping prey, ballooning, and prey interception and capture. Of these, orb webs deserve special mention. The typical orb web's architecture consists of a frame holding radii that support a spiral sticky thread, but there are many architectural variations of this basic layout. The typical web needs to absorb the energy of the intercepted prey and retain them long enough to give the spider time to locate and subdue them. Geometrically similar orb webs are constructed by the members of the superfamily Araneoidea and two cribellate families: Uloboridae and Deinopidae. Araneoidea includes approximately a quarter of described spider species among 17 families (World Spider Catalog, 2020) and has an appropriately impressive variation in web architectures. They include the characteristic orb webs (e.g., Araneidae, Tetragnathidae), as well as cob-webs (Theridiidae, Nesticidae) and sheet webs (e.g., Linyphiidae, Cyatholipidae), among others, such as those that have secondarily lost capture webs entirely (e.g., Mimetidae, Arkyidae). Most spiders, however, do not construct a web to intercept prey and

many make no foraging web whatsoever (Shear, 1986; Dimitrov et al., 2017; Fernández et al., 2018a, 2018b; Coddington et al., 2019).

The prevailing understanding of the phylogenetic relationships among spider species has changed over the past decades, sometimes gradually and sometimes drastically, but it is converging on a more stable, supported pattern. As data matrix sizes have increased – both in terms of terminals and loci – a number of novel relationships have become apparent. One of the most important of these regards the former cribellate orb-weaving superfamily Deinopoidea (Uloboridae + Deinopidae). Based on a number of data types and analyses, it is both no longer considered a monophyletic group nor closely related to Araneoidea, the ecribellate orb weavers, and thus refuting the Orbiculariae hypothesis which suggested that cribellate and ecribellate orb-weavers formed a lineage (Bond et al., 2014; Fernández et al., 2014; Dimitrov et al., 2017; Wheeler et al., 2017). While the stickiness of araneoid orb webs is achieved by the use of a unique type of visicid, gluey silk,  cribellate orb webs rely on a different type of sticky silk which is made of thousands of fine looped nanofibrils, and its adhesive properties are attained by a combination of mechanical interlock with the prey cuticle, adhesion to insect cuticular wax via capillary,  hygroscopic, and van der Waals forces (Opell, 2013; Bott et al., 2017). Recent analyses have suggested that cribellate orb-weavers are more closely related to members of the Retrolateral Tibial Apophysis (RTA) Clade (a diverse clade of largely cursorial and ambush spiders; most RTA members do not rely on webs to intercept prey) and the families Oecobiidae and Hersiliidae than to ecribellate orb-weavers (Bond et al., 2014; Garrison et al., 2016; Fernández et al., 2018a), as it was generally accepted until 2014 (e.g., Hormiga and Griswold, 2014). The grade of families subtending the RTA Clade – uloborids, deinopids, oecobiids, and

hersiliids, together termed the UDOH Grade – has been broadly supported but the relationships therein are inconsistent (Fernández et al., 2018a). Other changes in Mygalomorphae (a clade including tarantulas and their kin), Synspermiata (a clade of ecribellate spiders with simple genitalia including spitting spiders, cellar spiders, and others), and within both Araneoidea and the RTA Clade have led to a critical eye being cast on relationships both old and new (Kallal et al., 2018; Kuntner et al., 2019; Michalik et al., 2019; Opatova et al., in press).

As the datasets have grown from a handful to hundreds or thousands of loci with the adoption of modern sequencing methods, the spider tree of life is coming into sharper focus. However, the long legacy of Sanger sequencing data has resulted in a taxon sampling which dwarfs that of high throughput sequencing methods, even at the family level, thus far resulting in trees missing numerous branches needed to answer long-standing questions about spider biology. Over the past five years, both the overall number of taxa and taxon specificity (e.g., family-level) of analyses of spider interfamilial relationships have increased (e.g., Garrison et al., 2016; Cheng and Piel, 2018; Fernández et al., 2018a; Hedin et al., 2018; Kallal et al., 2018; Shao and Li, 2018; Wood et al., 2018; Hedin et al., 2019; Kuntner et al., 2019; Michalik et al., 2019; Kulkarni et al., 2019; Opatova et al., in press). The increasing consensus has led to more resolved and robust trees at various phylogenetic scales, making comparative questions interpretable in new ways.

One of the perennial questions in spider biology involves the evolution and diversification of webs (Fig. 1) and has been the subject of some recent debate as new phylogenies revised our understanding of spider relationships (e.g., Fernández et al., 2018a, 2018b; Coddington et al.,

2019). While all spiders spin silk, how silk is used varies considerably across the spider tree of life. The types of capture webs have been coded and analyzed in increasingly sophisticated ways although a consensus on how to code and analyze these complex and interconnected type of data is lacking (Blackledge et al., 2009; Dimitrov et al., 2012; Garrison et al., 2016; Dimitrov et al., 2017; Fernández et al., 2018a, 2018b; Coddington et al., 2019; Dimitrov and Hormiga, submitted). This is not least because of imperfect comparative methods and simplification of a complex suite of behaviors into states based on resemblance of the final silken structure. While specific data on morphological and behavioral homologies may be ideal, they are absent for the vast majority of spider lineages. It is important to note that coding web architecture comes with a major caveat: a web is the result of a series of integrated behaviors, some of which can be homologized across species (e.g., the radius construction behavior in an orb web; Eberhard, 1982) or not (e.g., what would be the homolog of the radius construction behavior in a sheet web?). Up to this date, comparative biology analyses have treated web architecture as a phylogenetic character, with web types analyzed as alternative states, an approach that has been referred as a quantum leap of the concept of homology (Dimitrov and Hormiga, submitted) because webs are not, in and of themselves, homologous to each other (e.g., Eberhard, 2018). Accepting the treatment of variation in overall web architecture as a character brings us to additional difficulties, such as how to exactly code and analyze such variation into states with the goal of reconstructing ancestral webs. New methods using nested hidden states and structured Markov models (Tarasov, 2019) may be an important new tool to simultaneously account for the hierarchical and hidden processes addressing the absence or presence of webs and their diverse forms.

Questions regarding the phylogeny of spiders remain, mainly in the areas of sampling and analysis, and these must be resolved before tangling ourselves into further discussions about the origins and evolution of complex structures, such as webs. Approximately one quarter of spider families remain unsampled to date for transcriptomes, including one araneoid family which was not included in previous phylotranscriptomic works focusing on orb-weavers (Fernández et al., 2018a). Topologically, insufficient taxon sampling can lead to spurious relationships, sometimes stemming from long branch attraction (LBA) and other common artifacts in phylogenetic

inference. Such a phylogenetic hypothesis might not only have specious clades but also confound downstream comparative analyses related to ancestral trait reconstruction and diversification rate estimation. In the case of the former, conflicting signal made placement of Uloboridae difficult in Fernández et al. (2014), where the UDOH Grade was represented by only two terminals. Another example lies in speciation rate analyses, which rely on branch lengths and tree density. Garrison et al. (2016) indicated that multiple lineages, including the RTA Clade, Avicularioidea, and Araneoidea had elevated diversification rates, whereas increased sampling by Fernández et al. (2018a) produced a more nuanced picture by including more taxa. Rather than a basal speciation increase subtending Araneoidea, the families Theridiidae, Tetragnathidae, Linyphiidae, and Araneidae are specifically suggested to have a higher diversification rate relative to the other araneoid families. For these reasons, increasing taxon sampling is a fundamental aim.

The second assortment of issues to be examined relates to phylogenetic methods. The range of approaches used to analyze phylogenomic data is vast, with variations both subtle and substantial often unique to specific taxa or working groups. It is beyond the scope of this work to outline the numerous types of data and how they can be analyzed. Typical methodological differences may include orthology assessment, matrix occupancy, alignment trimming, tree inference methods, and model selection, all of which can have an effect on topologies with variable resemblance to each other. For instance, trimming has been shown to have deleterious effects on single locus trees (Tan et al., 2015) but this effect is believed to be overwhelmed by weight of signal in concatenated analyses (Philippe et al., 2017). In addition, some of the methods to calculate node support may be ill-equipped for matrices of phylogenomic scale; that is, are traditional measures

of support, such as bootstrapping, actually telling us as much when hundreds of loci and thousands of sites are analyzed? Some analyses suggest not (Kumar et al., 2012), and alternatives using concordance factors based on loci (Gadagkar et al., 2005; Ane et al., 2007) and sites (Minh et al., 2020) have been proposed.

Here, we infer a new phylogenetic hypothesis for Araneae with special emphasis on the ecribellate orb-weavers (Araneoidea), based on several hundred loci generated from transcriptome (RNA-Seq) data. Our taxon sampling greatly expands on previous works in an effort to understand more of the relationships among the main spider lineages. Analyses are conducted with varying orthology assessment methods, matrix occupancy, trimming, and tree inference approaches in order to explore their impact on the final hypothesis. We use the resulting topologies to reexamine two long-standing questions in spider evolution: the tempo and mode of divergences and the evolution and diversification of their webs.

MATERIAL AND METHODS

*Extraction and transcriptome sequencing*

New transcriptomic data were generated for 53 spider specimens, focusing on increasing taxon sampling in areas previously undersampled or unsampled. Voucher specimens and tissue for these animals are deposited at the Museum of Comparative Zoology at Harvard University. In addition to material sequenced previously (Bond et al., 2014; Fernández et al., 2014; French et

al., 2014; Sanggaard et al., 2014; Sharma et al., 2014; Zhao et al., 2014; Brewer et al., 2015;

Hedin, 2015; Meng et al., 2015; Garrison et al., 2016; Rix et al., 2017; Cheng and Piel, 2018;

Fernández et al., 2018a; Kallal et al., 2018; Shao and Li, 2018; Michalik et al., 2019), our

available taxon sampling includes 272 terminals, of which 263 are spiders (Supplement 1). This

sums to more than 100 additional taxa in comparison to the largest published dataset (Fernández

et al., 2018a). This full taxon sample of 272 terminals is henceforth the *all* dataset. The *all*

dataset includes representatives of 99 of 120 spider families (82.5%). Specifically, 13 of 21

mygalomorph families (61.9%) and 86 of 99 araneomorph families (86.9%) are represented. For

the first time in a phylogenomic work, representatives of all 17 araneoid families are included in

the analyses. To focus on resolving araneoid interfamilial relationships, we also analyzed a

reduced matrix comprised of 94 araneoids and six outgroup lineages (eresids, nicodamoids, and

the lycosid *Schizocosa rovneri*), which we call the *ara* dataset.

Extraction of mRNA and strand-specific cDNA library construction followed the protocols

described in Fernández et al. (2018a). New RNA-Seq sequences were generated using Illumina

HiSeq2500 (2 x 150 bp) technologies. Assembly, sanitation, and reading frame detection

pipeline are as in Fernández et al. (2018a) with the addition of running the perl script Rcorrector

(Song and Florea, 2015) for preassembly error correction and downstream efficiency.

*Orthology and matrix variations*

Orthology assessment was conducted using two methods: BUSCO (Simão et al., 2015) and

UPhO (Ballesteros and Hormiga, 2016). Single copy loci retrieved using BUSCO were used for

11

the *all* and *ara* datasets due to its relative ease of use, and it follows Fernández et al. (2018a).

UPhO delivered matrices with more missing data and lower locus counts in datasets with many

terminals, and so its use is limited to the *ara* dataset.


Orthology assessment using BUSCO was conducted by querying a list of hidden Markov model

profiles of putatively single copy arthropod amino acid loci. A maximum of 2,675 loci are

retrievable. The pipeline used here follows Fernández et al. (2018a) and Kallal et al. (2018). The

*all* dataset was tested at 1%, 50%, 67%, and 90% occupancy thresholds with and without

trimming. Multiple sequence alignment was conducted using MAFFT v7 (Katoh and Standley,

2013) and trimmed, if relevant, using trimAl v1.2 (Capella-Gutiérrez et al., 2009) with default

settings. For UPhO, the *ara* dataset was subjected to all-versus-all BLAST searches using an

expectation value threshold of e = 1 x 10-3. Homolog clustering was performed using MCL in an

inflation factor of 6 (van Dongen, 2000; Enright et al., 2002).  Homolog groups were aligned and

trimmed as above facilitated with the UPhO script paMATRAX+ (Ballesteros and Hormiga,

2016). Occupancy thresholds of 25%, 33%, and 50% were tested in UPhO, keeping in-paralogs

and other variations of the same taxon per ortholog group. These were culled subsequently to

include only the longest sequence when the ortholog groups were aligned and trimmed as

described above.


To examine the effects of trimming on the resulting phylogenetic hypotheses, trees were inferred

on matrices that had and had not been subjected to trimming via trimAl (Capella-Gutiérrez et al.,

2009). In a few cases where entire terminals were trimmed, analyses were conducted with both

the reduced taxon matrix and the full matrix.

*Tree inference*

Parsimony analyses were conducted using MPboot (Hoang et al. 2018b) with 1,000 bootstrap replicates in IQ-TREE v1.7-betaX (Minh et al., 2020). Accuracy and speed of bootstrap calculation in MPboot, which uses ultrafast bootstrapping (Hoang et al., 2018a) compared favorably to other methods. Maximum likelihood tree inference was conducted using IQ-TREE v1.6 (Nguyen et al., 2015), with the best-fit amino acid model of the supermatrix determined using ModelFinder, as implemented in IQ-TREE (Kalyaanamoorthy et al., 2017). Nodal support was estimated using ultrafast bootstrapping (Hoang et al. 2018a) and an SH-like approximate likelihood ratio test (Guindon et al., 2010). Individual gene trees were built using IQ-TREE v1.6, with each run 5–10 times with the highest likelihood tree kept, using the model JTT+G. The gene trees were then analyzed using ASTRAL-II v4.10.12 (Mirarab and Warnow, 2015) in a multispecies coalescence (MSC) framework, with quality and support determined by normalized quartet score and local posterior probabilities (Sayyari and Mirarab, 2016). Due to low sampling variance in traditional resampling resulting in inflated supports, we used gene concordance factors (gCF) and site concordance factors (sCF) as implemented in IQ-TREE v1.7-betaX (Minh et al., 2020). This metric determines the number of loci and sites that are reflected in the maximum likelihood topology. This was conducted on a subset of analyses that used both BUSCO and UPhO orthology assessment methods. Robinson-Foulds (RF) distances (Robinson and Foulds, 1981) were generated using IQ-TREE (Nguyen et al., 2015).

*Divergence dating*

Time calibration of large phylogenies can be a difficult prospect, with some coestimation methods scaling poorly and requiring subsampling or months (or years) of computing time (e.g., Laumer et al., 2019). Following Eberle et al. (2018) wherein a number of faster methods were tested, we selected treePL (Smith and O'Meara, 2012) to analyze these data. This non-parametric rate-smoothing penalized likelihood method performed favorably against MCMCtree (Yang, 2007) and RelTime (Tamura et al., 2012). The topology generated by Fernández et al. (2018a) was reevaluated using an expanded and revised fossil calibration in a recent review of spider fossils and their placement, wherein younger clade ages were found than in most phylogenies (Magalhães et al., 2020). These findings have been modified for use in this work using treePL, with fossil maxima using the lower bounds of the 95% confidence intervals determined by Magalhães et al. (2020) to prevent anomalously ancient divergences. A total of 29 fossils were used as calibration points on 26 nodes and are summarized in Supplement S18. 'Prime' and 'thorough' options were used to optimize the analyses, and cross validation was used to select the optimal smoothing parameter. The smoothing parameter penalizes rate heterogeneity across the tree; increase of smoothing value assumes lower rate heterogeneity and more clock-like mode of rate evolution. Following Eberle et al. (2018), penalized likelihood optimization iterations were increased from the default of 2 to 5, and the number of penalized likelihood simulated annealing was doubled from 5,000 to 10,000.

*Web evolution*

The coding of web architecture was modified from Fernández et al. (2018b) and Coddington et al. (2019); some of the mygalomorph entries were taken from Opatova et al. (in press) (see Supplemental File S16). Following the analyses of Fernández et al. (2018a, 2018b), we use two separate reconstructions to first address the origin of foraging webs (and orb webs in particular) and second, the diversification of web architectures. Our analyses follow an approach specifically developed to handle hierarchically nested characters/states using structured Markov models (SMM) and hidden states (Tarasov, 2019). This method was developed to handle cases where hierarchical dependency between phenotypic traits occurs, such as in the case of spider webs and their architecture: only when the web is present it can have architecture. Hierarchical dependencies result in inapplicable codings which cannot be analyzed properly using alternative approaches (Tarasov, 2019). To apply this method we scored two characters: one for the absence or presence of foraging webs, and a second for scoring whether the web is an orb or not. We then amalgamated these two characters following Tarasov (2019) and built several models with increasing complexity starting from a three-state one-rate model without hidden states to models with up to 14 hidden states and 15 transition rates. In this framework, hidden states within an observable state only imply that the evolution of the observable state is not Markovian. Thus, observable states should consist of two or more hidden states to describe trait evolution as a Markovian process and all hidden states (where present) should be interpreted as the corresponding observable states. Each model was run with a switch dependency on and off (see Tarasov, 2019) using the rayDISC function in the R package corHMM (Beaulieu et al., 2017; Paradis and Schliep, 2019). The "switch-on" type of dependencies arise from phenotypic dependencies between traits in which a hierarchically upstream trait switches on and off the downstream trait (e.g., if the web is absent, then the web architecture character is switched off

and does not evolve). For the purpose of comparison between different approximations to the

scoring of web absence, we also designed a model where web absence is treated as a third state

in a web architecture character as done in most previous analyses (e.g. Blackledge et al., 2009,

Garrison et al., 2016, Dimitrov et al., 2017, Fernández et al., 2018a, 2018b).   As an alternative

Coddington et al. (2019) have scored web presence and web architecture in two different

characters where "?" and reconstructed ancestral states for each of these characters

independently and the two reconstructions were visually interpreted together. Their approach,

however, does not jointly estimate the marginal likelihood for both characters at internal nodes

(although they show a hierarchical relationship). In addition, scoring taxa where the web is

absent is equivalent to polymorphic coding which implies that taxa with such scores are

interpreted as having some web architecture while they do not build foraging webs at all.

Because of these shortcomings and given that the SMM approach properly handles hierarchical

dependencies we have not analyzed web diversity as two characters as proposed by Coddington

et al. (2019). The second question – the diversification of web architectures – is addressed

scoring web types in 13 states instead of just two: brush sheet (1), irregular aerial sheet (2),

irregular ground sheet (3), stereotyped aerial sheet (4), cob-web (5), orb web (6), aerial silk tube

(7),  tubular silk-lined burrow with trap door(s) (8), irregular non-sheetlike tangle (9), terminal

line (10), pseudo-orb (11), burrow with collar door (12) and open burrow (13). While many

analyses essentially treat variation in webs as phylogenetic character(s) (i.e., a transformation

series) to be optimized on a tree, this approach involves a highly questionable expansion of the

concept of homology, albeit tacitly adopted by many authors (e.g., Blackledge et al. 2009;

Dimitrov et al. 2012; Bond et al. 2014; Dimitrov et al. 2017; Fernández et al. 2018a) (see

'Discussion'). Using this 13-states scoring scheme for web architecture and the additional web

presence/absence character, we evaluated a set of SMM with rates that vary from a single rate up to 15 different rates, with and without switch character dependency, and with and without a hidden state associated to the orb web state. Because models with higher number of parameters generally result in better likelihoods, in order to compare models performance and avoid over parameterization, for each model we calculated the corresponding Akaike information criterion (AIC) (Beaulieu et al., 2017; Paradis and Schliep, 2019) and BIC (Bayesian Information Criterion) values (see supplementary materials). We used BIC for model comparison as a recent study shows that AIC may be biased in a phylogenetic context (Susko and Roger, 2020). We should also note that some web codings are open to different interpretations rather than simply being "correct" or "incorrect." For example, the sheet webs of *Physoglenes puyehue* (Physoglenidae) are extremely similar to the webs of many species of Linyphiidae (Dimitrov et al., 2017, fig. 7; Arnedo et al., 2009, fig. 2), and in absence of any data on the web building behavior of physoglenids, we code its web as we have coded linyphiid webs (a stereotyped aerial sheet), while Coddington et al. (2019) code *Physoglenes* as having an irregular aerial sheet and linyphiids as having stereotyped aerial sheets.

RESULTS

*Matrix composition*

Analyses were conducted on matrices ranging in size from 12 to 2,661 loci and between 4,491 and 1,270,722 sites depending on the orthology assessment method, occupancy threshold, and trimming (Table 1). For BUSCO analyses of all spiders, the most compact matrix (90%

occupancy) had 76 loci, whereas the maximum matrix including all loci represented in at least

two terminals had 2,661 loci. For araneoids only, BUSCO analyses ranged from 12 (90%

occupancy) to 2,040 (33% occupancy) loci, and for UPhO, from 162 (50% occupancy) to 1,263

(33% occupancy) loci. When implemented, trimming reduced the matrix size by between one-

third to two-thirds (e.g., BUSCO on all spiders at 67% occupancy: 460,845 untrimmed, 221,014

trimmed).

| Dataset | Orthology assessment | Occupancy threshold | Loci | Sites |
|---|---|---|---|---|
| *all* | BUSCO | 1% | 2,665 | 1,270,722 |
| *all* | BUSCO | 50% | 1,409 | 526,007 |
| *all* | BUSCO | 67% | 598 | 221,014 / 460,845 |
| *all* | BUSCO | 90% | 76 | 33,187 / 66,518 |
| *ara* | BUSCO | 33% | 2,040 | 930,557 |
| *ara* | BUSCO | 50% | 1,458 | 624,653 |
| *ara* | BUSCO | 67% | 646 | 270,267 / 410,393 |
| *ara* | BUSCO | 90% | 12 | 4,491 |
| *ara* | UPhO | 25% | 1,263 | 438,670 / 837,626 |
| *ara* | UPhO | 33% | 589 | 184,895 / 386,958 |
| *ara* | UPhO | 50% | 162 | 37,043 / 70,599 |

*Phylogenetic analyses*

Model selection using ModelFinder selected 'JTT plus empirical frequencies' as the preferred

model for all analyses, additionally selecting a free rate parameter of between seven and ten,

which relaxes the assumption of the Gamma distribution in which four categories are insufficient

for fitting the data. All major spider clades (e.g., Mygalomorphae, Araneomorphae,

Synspermiata, Palpimanoidea, Entelegynae, Araneoidea, RTA Clade) were recovered by most of

the 33 phylogenetic analyses conducted (Figs. 2, 3). The araneoid family Symphytognathidae,

not represented in previous transcriptomic analyses, was supported as sister group to Anapidae,

the sister lineage to all other araneoid families except theridiids, which are the sister group of all

other Araneoidea. Within the UDOH Grade, lower occupancy matrices (1–67%) found

Deinopidae as sister lineage to the RTA Clade, with Hersiliidae + Oecobiidae sister lineage to

Deinopidae + the RTA clade, and Uloboridae sister lineage to all of these. In contrast, high

occupancy analyses (90%) found Uloboridae to be the sister group to the RTA Clade and

Deinopidae as the sister lineage to Hersiliidae + Oecobiidae.

Different topologies and their support values are summarized in Table 2. Lower occupancy

matrices resulted in topologies more akin to each other based on RF distances than those derived

from higher occupancy matrices. Trimming seemed to result in little difference compared to

other variations of the matrix in concatenation and slightly more so for MSC. Furthermore,

topologies were more similar (based on RF distances) for concatenation methods versus MSC

methods regardless of occupancy at lower thresholds. Such differences included concatenation

19

analyses supporting Eresidae as the sister lineage to Nicodamoidea + Araneoidea, whereas MSC analyses supported Araneoidea as sister lineage of Eresidae + Nicodamoidea. Concatenation analyses supported Cyatholipidae as sister lineage to Synaphridae; MSC supported cyatholipids as sister lineage to linyphioids (Linyphiidae + Pimoidae). Another relevant difference within Araneoidea was related to the tetragnathoids (Tetragnathidae, Mimetidae and Arkyidae) and their relatives. MSC analyses found Mysmenidae as sister group to the clade including Malkaridae, Arkyidae, Mimetidae, and Tetragnathidae, but concatenation analyses determined Malkaridae as sister group to the remaining taxa, or Malkaridae + Mysmenidae sister clade to tetragnathoids (BUSCO and UPhO, respectively). In most cases, the alternatives had high local posterior probabilities and bootstrap scores.

| Clade | Method | UFB (Tr/Un) | SH-aLRT | gCF | sCF | LPP (Tr/Un) |
|---|---|---|---|---|---|---|
| NIC + ARA | B | 100/100 | - | 5.74 | 33 | (Ere, NIC): 0.98/0.97 |
| Ana + Sym | B | 100/100 | - | 14.7 | 35.9 | 1/1 |
| Mal + Mys | B | 97/91 | - | 4.87 | 29.4 | Tr: (Mys, (Mal, Tet)): 0.96; |
|  |  |  |  |  |  | Un: ((Mys, (Mal, Tet)): 0.5 |
| Syn + Phys | B | 100/100 | - | 4.41 | 33.3 | (Syn, (The, Ara)): 0.57/0.64 |
| The + Ara | B | 100/100 | - | 11.6 | 35.7 | 1/1 |
| NIC + ARA | U | 99/98 | 98.3/98.6 | 24.5 | 31.6 | (Ere, NIC): 0.83/0.87 |
| Ana + Sym | U | 100/100 | 100/100 | 2.93 | 35.6 | 1/1 |
| Mal + (Mys + Tet) | U | 100/100 | 100/100 | 4.41 | 34.9 | (Mys, (Mal, Tet)): 1/1 |
| Mys + Tet | U | 100/99 | 99.3/99.6 | 1.01 | 29.1 | (Mal, Tet): 0.93/0.99 |
| Syn + Nes | U | 100/100 | 100/99.8 | 11.2 | 30.4 | Tr: (Syn, (Nes, Phy)): 0.8; |
|  |  |  |  |  |  | Un: (Syn, ((Nes,Phy), (The,Ara))): 0.61 |
| The + Ara | U | 100/100 | 100/100 | 24.5 | 36.5 | 1/1 |

1   Additional differences in tree topology were found using the different orthology assessment

2   methods. In addition to the differences related to tetragnathoids (including tip-level differences

3   within Tetragnathidae and Mysmenidae, Figs. 3a, 3c), the placement of Synotaxidae differed

4   between analyses. Using BUSCO, *Synotaxus* was sister lineage to Physoglenidae (Fig. 3a),

5   whereas UPhO determined *Synotaxus* to be the sister group of Nesticidae (Fig. 3d). Different

6   topologies were also detected in the family Araneidae. Argiopinae (*Argiope* + *Cyrtophora*) was

7   not monophyletic in BUSCO analyses but it was monophyletic using UPhO; additionally, there

8   were various changes in the sister group to gasteracanthines (Figs. 3a, 3e). Additional topologies

9   with full support are available at the Harvard Dataverse repository. Trimming did not have an

10  appreciable effect on topology. The RF distances were lower between untrimmed and trimmed

11  MSC analyses (RF = 32) than concatenation (RF = 44), less than half of the difference between

12  MSC and concatenation regardless of trimming done (RF = 92–98).

13

14  For most nodes, we found uniformly high ultrafast bootstrap support. Concordance factor values,

15  however, varied widely, with gCFs lower than their respective sCFs. Where present, low

16  bootstrap support coincided with low concordance factor values. Furthermore, approximately

17  90% of the nodes had full bootstrap support despite concordance factors ranging from zero to

18  100. Even in well established clades, concordance values do not approach the uniformly high

19  bootstrap support (for gCF and sSCF, respectively, in BUSCO analysis with 67% occupancy;

20  S14): Opisthothelae (49.6, 39.6), Mygalomorphae (56.8, 44.3), Araneomorphae (43.3, 38.7),

21  Synspermiata (41.1, 42.7), Palpimanoidea (13.7, 37.7), RTA Clade (37.0, 50.4), and Araneoidea

22  (26.5, 40.1). Within Araneoidea, there is a similar pattern, with even congenerics' concordance

23  factor scores varying (S14, S15). For instance, *Trichonephila edulis* and *T. plumipes* were scored

24   (47.0, 63.6) and (55.0, 50.3) in the preferred BUSCO and UPhO analyses; *Theridiosoma*

25   *gemmosum* and *T. savannum* scored (80.9, 75.2) and (97.7, 73.8).

26       Parsimony analyses differed minimally from model-based analyses, except in two key

27   areas. First, in the analysis on the *all* dataset, Eresidae and Nicodamidae form a clade (UFBoot =

28   91), which is in turn sister group to the UDOH Grade + RTA Clade (UFBoot = 58) rather than

29   Araneoidea (S16). Second, the symphytognathoid families Anapidae, Mysmenidae,

30   Symphytognathidae, and Synaphridae form a clade, sister group to all other araneoid families

31   except Theridiidae (S16, S17). Theridiosomatidae is a sister group to Araneidae as in model-

32   based analyses (UFBoot = 98 and 95 on *all* and *ara* datasets, respectively).

33

a)

*Limulus polyphemus*
*Tachypleus tridentatus*
*Chaerilus celebensis*
*Pandinus imperator*
*Urodacus planimanus*
*Damon variegatus*
*Phrynus marginemaculatus*
*Mastigoproctus giganteus*
*Stenochrus* cf. *portoricensis*
*Liphistius malayanus*
*Liphistius* sp.

Mesothelae

Mygalomorphae

*Atypus* cf. *heterothecus*
*Sphodros rufipes*
*Megahexura fulva*
*Aliatypus coylei*
*Antrodiaetus unicolor*
*Porrhothele* sp.
*Cethegus fugax*
*Microhexura montivaga*
*Actinopus* sp.
*Damarchus* sp.
*Trichopelma laselva*
*Acanthoscurria geniculata*
*Aphonopelma iviei*
*Macrothele calpeiana*
*Paratropis* sp.
*Calisoga longitarsis*
*Pionothele* sp.
*Stanwellia* sp.
*Cyclocosmia truncata*
*Hebestatis theveneti*
*Aptostichus stephencolberti*
*Promyrmekiaphila clathrata*
*Idiops bersebaensis*
*Euoplos* sp.
*Idiosoma* sp.
*Cataxia* sp.

*Hypochilus gertschi*
*Hypochilus pococki*
*Pikelinea* sp.
Prithinae sp.
*Filistata insidiatrix*
*Kukulcania hibernalis*

Synspermiata

*Trogloraptor marchingtoni*
*Calponia harrisonfordi*
Caponiidae sp.
*Ariadna* sp.
*Segestria* sp.
*Segestria bavarica*
*Tasmanoonops* sp.
*Maoriata* sp.
Orsolobidae sp.
*Dysdera crocata*
*Costarina* sp.
*Ischnothyreus* sp.
*Opopaea* sp.
*Telema tenella*
*Telema cucurbitina*
*Singaporemma bifurcata*
*Diguetia* sp.
*Plectreurys* sp.
*Pholcus manueli*
*Pholcus phalangioides*
*Althepus christae*
*Flexicrurum* sp.
*Drymusa* sp.
*Periegops suterii*
*Loxosceles deserta*
*Loxosceles rufescens*
*Ochyrocera* sp.
*Stedocys* sp.
*Scytodes globula*
*Scytodes thoracica*

*Archoleptoneta* sp.
*Calileptoneta californica*
*Leptoneta foliiformis*
*Austrochilus forsteri*
*Hickmania troglodytes*
*Progradungula otwayensis*
*Tarlina* sp.
*Gradungula sorenseni*
*Pianoa isolata*

Palpimanoidea

*Huttonia palpimanoides*
*Austrarchaea* sp.
*Mecysmauchenius* sp.
*Colopea* sp.
*Otiothops birabeni*
*Palpimanus gibbulus*

0.1

c)

a

b

b)

UDOH Grade

*Sybota* sp.
*Miagrammopes* sp.
*Zosis* sp.
*Philoponella herediae*
*Uloborus glomosus*
*Hersilia* sp.
*Tamopsis* sp.
*Ypypuera* sp.
*Uroctea durandi*
*Oecobius cellariorum*
*Oecobius navus*
*Menneus* sp.
*Deinopis* sp.
*Deinopis longipes*

RTA Clade

*Cybaeodamus taim*
*Forsterella* sp.
*Caayguara ybytyriguara*
*Heteropoda* sp.
*Amaurobius ferox*
*Callobius* sp.
*Agelenopsis emertoni*
*Agelenopsis pennsylvanica*
*Dictyna sancta*
*Calymmaria* sp.
*Calymmaria persica*
*Cicurina travisae*
*Cicurina vobora*
*Cycloctenus* sp.
*Neoramia* sp.
*Badumna longinqua*
*Paramatachia* sp.
*Amphinecta* sp.
*Metaltella simoni*
*Cambridgea* sp.
*Corasoides* sp.
*Homalonychus theologus*
*Rebilus* sp.
*Hibana* sp.
*Clubiona* sp.
*Clubiona trivialis*
Liocranidae sp.
*Sergiolus capulatus*
*Trachelas tranquillus*
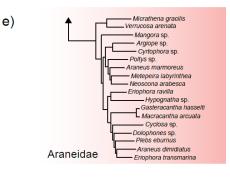*Molycria* sp.
*Anzacia* sp.
*Lampona* sp.
*Odo patricius*
*Tibellus oblongus*
*Metacyrba taeniola*
*Habronattus signatus*
*Habronattus ustulatus*
*Falconina gracilis*
*Nyssus* sp.
*Karaops raveni*
*Teminius* sp.
*Zora* sp.
*Uliodon* sp.
*Tengella radiata*
*Senoculus* sp.
*Oxyopes* sp.
*Peucetia longipalpis*
*Sidymella* sp.
*Aphantochilus* sp.
*Misumenoides formosipes*
*Thomisus spectabilis*
*Ctenus corniger*
*Anahita punctulata*
*Phoneutria fera*
*Psechrus singaporensis*
*Fecenia protensa*
*Fecenia* cf. *travancoria*
*Dolomedes triton*
*Architis tenuis*
*Nilus albocinctus*
*Pisaurina mira*
*Sphedanus quadrimaculatus*
*Cupiennius coccineus*
*Cupiennius salei*
*Sossipus placidus*
*Hippasa holmerae sundaica*
*Allocosa alticeps*
*Pardosa pseudoannulata*
*Lycosa* sp.
*Schizocosa rovneri*

Eresidae, Nicodamoidea,
& Araneoidea

a)

*Gandanameno* sp.
*Eresus walckenaeri*
*Stegodyphus mimosarum* — Eresidae
*Megadictyna thilenii* — Megadictynidae
Nicodamidae sp. 1
Nicodamidae sp. 2 — Nicodamidae — Nicodamoidea

*Latrodectus hasselti*
*Latrodectus tredecimguttatus*
*Ariamnes colubrinus*
*Euryopis* sp.
*Anelosimus eximius*
*Parasteatoda tepidariorum*
*Theridion* sp. — Theridiidae

*Anapistula* sp. GH2585
*Anapistula* sp. GH2596
*Patu* sp.
*Patu* sp. GH2575 — Symphytognathidae

*Anapisona hamigera*
*Anapis* sp. GH2392
*Anapis* sp. GH2582
Anapidae sp. 144904
*Novanapis* sp.
*Queenslanapis* sp.
*Maxanapis burra*
*Spinanapis* sp. — Anapidae

*Pararchaea alba*
*Malkara* sp. 17
Malkaridae sp. 9
*Perissopmeros* sp. — Malkaridae

*Mysmenopsis ischnamigo*
*Maymena ambita*
*Mysmena leichardti*
*Microdipoena guttata*
*Mysmenella jobi*
Mysmenidae sp. GH2606 — Mysmenidae

(c)

*Gelanor* sp.
*Australomimetus* sp.
*Ero leonina* — Mimetidae

*Arkys* sp.
*Demadiana* sp. — Arkyidae

*Tetragnatha tantalus*
*Chrysometa eugeni*
*Nanometa trivittata*
*Leucauge venusta*
*Azilia guatemalensis*
*Dolichognatha pentagona*
*Meta ovalis* — Tetragnathidae

*Cepheia longiseta* — Synaphridae

*Matilda* sp.
*Teemenaarus silvestris*
*Tekella* sp.
*Tekelloides* sp. 1
*Tekelloides* sp. 2 — Cyatholipidae

*Pimoa* sp. 1
*Pimoa* sp. 2 — Pimoidae

*Weintrauboa contortipes*
*Laminacauda parvipalpis*
*Neomaso* sp.
*Graphomoa theridioides*
*Frontinella communis*
*Novafroneta gladiatrix* — Linyphiidae

Physoglenidae sp.
*Physogelenes* sp.
*Meringa* sp.
*Runga* sp. — Physoglenidae

*Synotaxus* cf. *turbinatus* — Synotaxidae

*Nesticus cellulanus*
*Nesticus bishopi*
*Nesticus cooperi* — Nesticidae

*Epeirotypus chavarria*
*Naatlo* sp.
*Ogulnius* sp.
*Baalzebub* sp.
*Theridiosoma gemmosum*
*Theridiosoma savannum* — Theridiosomatidae

(d)

*Zygiella x-notata*
*Deliochus humilis*
*Phonognatha graeffei*
*Herennia multipuncta*
*Trichonephila clavipes*
*Trichonephila edulis*
*Trichonephila plumipes*
*Micrathena gracilis*
*Verrucosa arenata*
*Cyrtophora* sp.
*Poltys* sp.
*Argiope* sp.
*Mangora* sp.
*Neoscona arabesca*
*Metepeira labyrinthea*
*Araneus marmoreus*
*Hypognatha* sp.
*Eriophora ravilla*
*Gasteracantha hasselti*
*Macracantha arcuata*
*Araneus dimidiatus*
*Cyclosa* sp.
*Plebs eburnus*
*Dolophones* sp.
*Eriophora transmarina* — Araneidae

(e)

0.1

b)

c)

Malkaridae
*Mysmenopsis ischnamigo*
*Maymena ambita*
*Mysmena leichardti*
*Microdipoena guttata*
*Mysmenella jobi*
Mysmenidae sp. GH2606
Mysmenidae
Mimetidae
Arkyidae
*Tetragnatha tantalus*
*Chrysometa eugeni*
*Nanometa trivittata*
*Leucauge venusta*
*Azilia guatemalensis*
*Dolichognatha pentagona*
*Meta ovalis*
Tetragnathidae

d)
Physoglenidae sp.
*Physogelenes* sp.
*Meringa* sp.
*Runga* sp.
Physoglenidae
Synotaxidae
Nesticidae

e)
*Micrathena gracilis*
*Verrucosa arenata*
*Mangora* sp.
*Argiope* sp.
*Cyrtophora* sp.
*Poltys* sp.
*Araneus marmoreus*
*Metepeira labyrinthea*
*Neoscona arabesca*
*Eriophora ravilla*
*Hypognatha* sp.
*Gasteracantha hasselti*
*Macracantha arcuata*
*Cyclosa* sp.
*Dolophones* sp.
*Plebs eburnus*
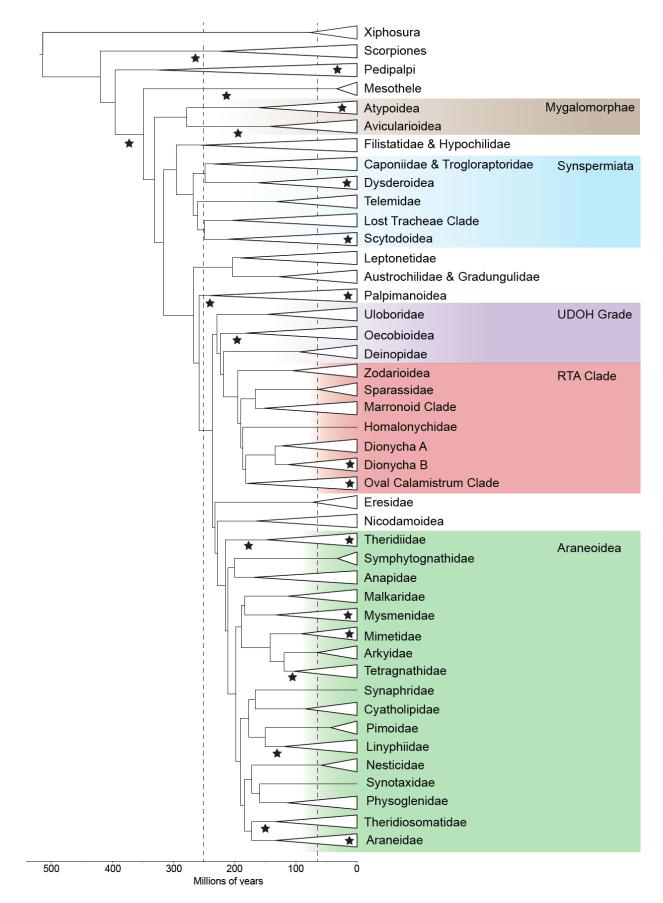*Araneus dimidiatus*
*Eriophora transmarina*
Araneidae

35

36

37

38 *Divergence dating*

39

40 Cross-validation in treePL selected the default smoothing factor of 100. Divergence dates

41 inferred using treePL are depicted in Fig. 4. The last common ancestor of spiders and Pedipalpi

42 occurred approximately 396 Ma, and the last common ancestor of Mesothelae and Opisthothelae

43 occurred approximately 350 Ma. Mygalomorphae and Araneomorphae last shared a common

44 ancestor 331 Ma. Within Araneoidea, families diverged from their sister lineages 120–215 Ma,

45 with Arkyidae + Tetragnathidae being the youngest and Theridiidae + other araneoids being the

46 oldest.

47

Xiphosura
Scorpiones
Pedipalpi
Mesothele
Atypoidea
Avicularioidea
Mygalomorphae
Filistatidae & Hypochilidae
Caponiidae & Trogloraptoridae
Synspermiata
Dysderoidea
Telemidae
Lost Tracheae Clade
Scytodoidea
Leptonetidae
Austrochilidae & Gradungulidae
Palpimanoidea
Uloboridae
UDOH Grade
Oecobioidea
Deinopidae
Zodarioidea
RTA Clade
Sparassidae
Marronoid Clade
Homalonychidae
Dionycha A
Dionycha B
Oval Calamistrum Clade
Eresidae
Nicodamoidea
Theridiidae
Araneoidea
Symphytognathidae
Anapidae
Malkaridae
Mysmenidae
Mimetidae
Arkyidae
Tetragnathidae
Synaphridae
Cyatholipidae
Pimoidae
Linyphiidae
Nesticidae
Synotaxidae
Physoglenidae
Theridiosomatidae
Araneidae

500    400    300    200    100    0
Millions of years

48

49

50    *Web evolution*

51

52    The different SMM models used in the ancestral state reconstruction analyses and the relevant

53    statistics are summarized in Table (S22). Several models scored closely when using reduced

54    scoring for the web architecture. A model where we allowed for one hidden state for the orb web

55    character and two rates scored marginally, but not significantly (BIC difference < 2), better than

56    the second best model. This model, as well as most of the best scoring models from the analyses

57    of the two states web architecture dataset, supports five independent origins of the orb webs:

58    three in Araneoidea, once in Deinopidae, and once in Uloboridae (Figs. 5, S20). There are

59    multiple instances of web loss within and outside araneoids and support for the presence of a

60    web as the ancestral condition for spiders (as in Fernández et al., 2018a, 2018b). The analysis of

61    the dataset with fine grain scoring of web architectures (13 states) also supports multiple origins

62    of orb webs but it differs in that it suggests a single origin of orb webs in Araneoidea (Figs. 5,

63    S21). Tubular silk-lined burrow with trap door(s) is inferred as the ancestral web type for spiders

64    and multiple losses of web from different ancestral web types are inferred across the phylogeny.

65    In the 13-state analyses we found two models that scored very closely with only a marginal

66    difference in their BIC values, however the inferred evolution of web architecture under these

67    two models does not differ and here we present the result of the model with the best BIC (Fig. 5).

68    Analyses of both the two and the 13-state dataset support multiple instances of transitions from

69    webless foraging to webs in the RTA Clade and a single loss of webs in the ancestor of this

70    group. When we tested models with an increasing number of hidden states for the non-orb web

71    state in the two state web architecture results converged to those of analyses of the 13-state

72    dataset when hidden character spaces was increased to 11. Only two models of all those tested

73    inferred a single origin of orb webs as hypothesized by the ancient orb hypothesis but those were

74    significantly worse than any of the models suggesting multiple origins (BIC differences were

75    higher than 30 in favour of models resulting in multiple origins inference).

76

81  DISCUSSION

82

83  *Spider phylogeny*

84

85  Our study, with strategically increased taxon sampling to maximize web diversity across lineages

86  and a variety of analytical methods produced a well-resolved spider tree of life. For the

87  overlapping taxa, results recovered most of the phylogenetic relationships established by

88  previous works (Garrison et al., 2016; Dimitrov et al., 2017; Wheeler et al., 2017; Cheng and

89  Piel, 2018; Fernández et al., 2018a; Hedin et al., 2019; Kallal et al., 2018; Shao and Li, 2018;

90  Kulkarni et al., 2019; Michalik et al., 2019), reinforcing several previous topologies. For this

91  reason, we limit our discussion of relationships to highlight places in which our results are novel.

92

93  Within Mygalmorphae, we found the typical atypoid – avicularioid split within Mygalomorphae.

94  A notable difference compared to recent work on this clade by Fernández et al. (2018a) and

95  Hedin et al. (2019) involves the placement of Dipluridae and Porrhothelidae; we find them as

96  sister lineages, as the earliest diverging clade with Avicularioidea. The analyses of Fernández et

97  al. (2018a) did not place *Porrhothele* with good support, whereas Hedin et al. (2018) placed this

98  taxon more distally, sister to a clade including Macrothelidae, Nemesiidae, Halonoproctidae,

99  Atracidae, and Actinopodidae. The more densely sampled mygalomorph analyses of Opatova et

100 al. (in press) show porrhothelids as early diverging avicularioids and diplurids in the fraught

101 clade including nemesiids and close relatives.  Our analyses place *Actinopus* as an early

102 diverging avicularioid near theraphosids whereas actinopodids are sister lineage to atracids in

103 Hedin et al. (2018) and Opatova et al. (in press).

104

105    Within Synspermiata, relationships are similar to other works on the group (e.g., Michalik et al.,

106    2019), with monophyly for the major clades Dysderoidea, Scytodoidea, and the Lost Tracheae

107    Clade. Notably, Ochyroceratidae and Psilodercidae are not closely related, a proposal initially

108    based on morphology (Wunderlich 2008) but not supported conclusively by molecular data (the

109    analysis of Wheeler et al. 2017 places 'cf. *Psiloderces*' in Ochyroceratidae with weak support).

110    Plectreuridae is placed in the Lost Tracheae Clade with tetrablemmids and pholcids, following

111    Wheeler et al. (2017) and Shao and Li (2018). Additionally, Oonopidae rather than Orsolobidae

112    is the sister group of Dysderidae, *contra* the results of Fernández et al. (2018a). In the

113    superfamily Palpimanoidea (trapjaw spiders, pelican spiders, and their kin), all five families are

114    represented, but relationships differ from those of Fernández et al. (2018a) as well as

115    palpimanoid-specific analyses using Sanger markers and morphology (Wood et al. 2012) or

116    UCEs (Wood et al. 2018, Kulkarni et al. 2019). Our taxon sampling is more limited than that of

117    Wood et al. (2018),  and the degree of difference suggests sampling, data type, and analysis type

118    are very important for resolving palpimanoid relationships.

119

120    Most analyses (see above) place Uloboridae as sister lineage to a clade that includes all other

121    UDOH families (Hersilidae, Oecobiidae and Deinopidae) and the RTA lineages. Hersiliidae and

122    Oecobiidae are always sister lineages (Oecobioidea). This is consistent with the results of

123    Fernández et al. (2018a) and contrary to the results of Shao and Li (2018), in which eresids were

124    placed in the UDOH Grade. Within the RTA Clade, additional taxa change little of the

125    relationships established by previous works focusing on this group (e.g., Cheng and Piel, 2018).

126    The non-monophyly of Ctenidae is supported, following other recent works (Wheeler et al.,

127    2017; Piacentini and Ramírez, 2019). In Fernández et al. (2018a), the zoropsids *Tengella* and

128    *Uliodon* were sister groups but not strongly supported; here, they are not supported as sister

129    lineages and Zoropsidae is not monophyletic. The senoculid branch is very long (as in Fernández

130    et al. 2018a); this may be an artifact due to a relatively low BUSCO count, and its placement

131    varies in our analyses.

132

133    The majority of analyses also corroborate Nicodamoidea as the sister lineage of Araneoidea as

134    suggested by Dimitrov et al. (2012, 2017), Wheeler et al. (2017) and Fernández et al. (2018a).

135    Some analyses place Eresidae as sister group to the nicodamoids and/or as sister lineage to

136    UDOH Grade + RTA Clade, but most place eresids as sister lineage to Araneoidea +

137    Nicodamoidea. All but parsimony analyses differed from the results of Kulkarni et al. (2019) in

138    this way. The earliest diverging araneoid lineage is Theridiidae, differing from Fernández et al.

139    (2018a) where it was sister group to Anapidae which were in turn sister lineage to all remaining

140    araneoids, but consistent with the results of Dimitrov et al. (2012) using Sanger data and

141    Kulkarni et al. (2019) using UCEs. The newly included araneoid family Symphytognathidae is

142    sister group to Anapidae in virtually all analyses; symphytognathids were not represented in

143    Fernández et al. (2018a), which may explain the placement of Anapidae as sister to Theridiidae.

144    Anapidae and Symphytognathidae are the only two symphytognathoid families to form a clade

145    based on model-based transcriptomic data. Parsimony analyses showed a monophyletic

146    symphytognathoid group (sans Theridiosomatidae), a result strikingly similar to the UCE-based

147    analyses by Kulkarni et al. (2019) where the symphytognoid families are resolved as a clade. The

148    UCE datasets that support symphytognathoid monophyly happen to have low occupancy

149    (<50%), with more loci but also more missing data than datasets with higher occupancy.

150

151 Malkaridae and Mysmenidae are placed near the base of the tetragnathoid clade, but their

152 positions vary. Their phylogenetic placement has key implications for the evolution of the

153 capture web given that malkarids, arkyids, and mimetids do not spin foraging webs (Framenau et

154 al., 2010; Benavides et al., 2017; Hormiga and Scharff, 2020) whereas webs are found in

155 mysmenids and tetragnathids (see web discussion below). Within Tetragnathidae, *Chrysometa*

156 and *Nanometa* are closely related in many analyses, a relationship suggested by morphological

157 data but lacking in Sanger-based molecular analyses (Álvarez-Padilla and Hormiga, 2011;

158 Álvarez-Padilla, et al. 2020). The rogue taxon *Azilia* remains resistant to stable placement and is

159 the sister taxon to either leucaugines or metaines depending on the analysis. Likewise, *Cepheia*

160 (the sole representative of the family Synaphridae in our analyses) is typically placed as sister

161 group to cyatholipids, but is found in a more basal location or near other symphytognathoids in

162 other analyses, an issue perhaps solvable by including additional representatives of this small

163 family (with only three genera and 13 described species). Physoglenids, nesticids, and synotaxids

164 form a clade. Finally, all analyses find Theridiosomatidae and Araneidae as sister lineages

165 including both model-based and parsimony analyses. Within Araneidae, the Phonognathinae

166 lineage is sister to Nephilinae + remaining araneids. Short internodes in the araneid clade sister

167 to gasteracanthines continue to evade resolution.

168

169 *Methodology and support values*

170

171 Notably, the more conserved loci from BUSCO, where they differed from UPhO, presented

172 differences at more recent splits. For instance, morphology and Sanger-based data have nearly

173    always supported a close relationship between argiopine and cyrtophorine araneids (in fact,

174    combined into Argiopinae in Scharff et al. 2020), but *Argiope* and *Cyrtophora* were not sister

175    lineages in numerous BUSCO-based analyses. This suggests the utility of orthologs inferred with

176    BUSCO, while functional at all levels, may be best at a deeper timescale. We also found the

177    occupancy threshold could be raised higher using BUSCO than UPhO before returning

178    anomalous results, but both were fairly consistent when provided with sparse matrices. The

179    minimal occupancy BUSCO matrix was less different topologically from the 67% occupancy

180    analyses than concatenation was from MSC analyses of the same occupancy (based on RF

181    distances). This indicates that, for this dataset, the phylogenetic signal is more robust to the

182    presence of missing data than to tree inference method. Furthermore, we found that robustness to

183    trimming was comparable using both concatenation and MSC methods. This furthers Philippe et

184    al.'s (2017) statement of signal overwhelming trimming effects using concatenation but also for

185    coalescence-based methods, despite single locus tree issues found by Tan et al. (2015).

186

187    We found that bootstrap support and SH-aLRT support seemed to covary, but concordance

188    factors differed considerably. The use of concordance factors (Minh et al. 2020) gives additional

189    value to inflated bootstrap supports common in many phylogenomic analyses. Given that

190    concordance factors do not have a generally recognized threshold of acceptable support (and

191    indeed may never have such a threshold given how predicated they are on the number of sites

192    and loci), they can be difficult to interpret. Interestingly, many relationships that are strongly

193    supported by previous morphological and molecular works with high support found little

194    corroboration in gCF and sCF analyses. For instance, only about one third of loci supported well-

195    established hypotheses like the monophyly of Pimoidae + Linyphiidae (e.g., Arnedo et al., 2009;

196    Dimitrov et al. 2017) or the monophyly of Araneidae including nephilines (e.g., Kallal et al.

197    2018; Scharff et al. 2019). Perhaps worryingly, this suggests that many relationships supported

198    via bootstrapping could mask conflict with other nearly as frequent relationships.

199

200    Recent advances in understanding spider interfamilial relationships have come from two

201    different types of phylogenomic data. While transcriptomes are the more common data type in

202    spider phylogenetics (e.g., Garrison et al., 2016; Cheng and Piel, 2018; Fernández et al. 2018a;

203    Kallal et al., 2018), target capture methods are increasingly used (e.g., Hedin et al., 2018; Wood

204    et al., 2018, Hedin et al. 2019; Kulkarni et al., 2019; Opatova et al., in press). In a study with a

205    similar scope as this, Kulkarni et al. (2019) used UCEs to build a spider phylogeny with

206    considerable overlap but also concerning conflict in the results. The symphytognathoid

207    assemblage, which comprises Anapidae, Symphytognathidae, Mysmenidae, and

208    Theridiosomatidae (Griswold et al., 1998) and sometimes Synaphridae (Lopardo et al., 2010; not

209    sampled in Kulkarni et al. 2019) was found to be monophyletic in that UCE dataset – a result not

210    recovered in any other analysis using molecular data, but supported by morphology. Previous

211    studies using transcriptomes for three of these four families (analyzed as amino acids only) found

212    no support for close relationships among them (Fernández et al. 2018a). Another notable

213    incongruence with the UCE hypothesis is offered by the placement of Nicodamoidea, a small

214    clade that includes the families Nicodamidae and Megadictynidae, which is sister group to

215    Araneoidea with transcriptomes (Fernández et al., 2018a) whereas it is sister group to Eresidae

216    with UCEs (Kulkarni et al., 2019). The reason for this perplexing discrepancy remains to be fully

217    understood.

218

219    The loci revealed by transcriptomes are exclusively coding in nature and evolve at varying rates,

220    while UCEs are ultraconserved regions composed of exons as well as introns. Hedin et al. (2019)

221    showed that the UCEs targeted using the Arachnida probe set are mostly exonic and multiple

222    UCE loci may target different regions of the same gene. This finding makes both data types

223    comparable in a way that they both are coding, however UCEs can then be viewed as a subset of

224    transcriptomes.

225

226    Transcriptomes are generally subjected to tree-building algorithms as amino acids whereas UCEs

227    are analyzed as nucleotide data. The third nucleotide in synonymous codons might contain

228    phylogenetic signal, however such information is masked in case of transcriptomes.

229    Additionally, transcriptomic data are subjected to orthology assessment, however the same

230    methods are not used with the UCE data prior to phylogenetic analysis. Instead, the duplicate

231    removal step in the Phyluce pipeline (Faircloth, 2016) is assumed to filter out paralogs. Both data

232    types are genome scale in size and the highly supported conflicting relationships are implausible

233    since the bootstrap support is mostly >95 for large scale datasets; that is, one or both of such

234    hypotheses must be erroneous. Future analytical comparison is therefore warranted to understand

235    the conflict between these data types.

236

237    *Web evolution*

238

239    An increasing number of studies have relied on recent advances in spider phylogeny to

240    reconstruct the evolution and diversification of webs across Araneae. Following Blackledge et al.

241    (2009), recent analyses by Garrison et al. (2016) and Fernández et al. (2018a) coded nine and ten

242    types of webs respectively, with the latter study specifically coding capture webs plus a

243    simplified variable with three states addressing orb web origins. Fernández et al. (2018a)

244    specifically coded foraging webs, which are directly used to capture prey, although we lack a

245    precise and universally accepted definition, if such a thing is feasible, of what exactly a

246    "foraging web" is. Not surprisingly, both studies found webs to be ancestral for Araneae

247    (Garrison et al., 2016: Fig 6; Fernández et al., 2018a: Fig. S2), but the former inferred a single

248    origin for orb webs whereas the latter found multiple (ranging from two to six origins).

249    Fernández et al. (2018a) used two different characters to first, reconstruct the origin of webs

250    (including orb webs) and second, the diversification of web architectures, consequently it is not

251    appropriate to use their second reconstruction to address the first question. The assertions that

252    Fernández et al. (2018a) concluded that "the ancestral spider spun no foraging web" and that

253    "spider webs evolved *de novo* 10–14 times", repeatedly made by Coddington et al. (2019), are

254    inaccurate and easily refuted by the aforementioned study itself: Fernández et al.'s Figure S2

255    clearly shows the state "web (non-orbicular)", represented by a green circle, as ancestral for

256    Araneae.

257

258    Using an alternative coding scheme to deal with the absence of foraging webs, along with a

259    number of scoring changes correcting errors or providing alternative interpretations of web

260    types, Coddington et al. (2019) reassessed the Fernández et al. (2018a) data, finding a single

261    origin of the orb web (the "ancient origin hypothesis") but repeated independent losses of a

262    foraging web in all lineages of the large RTA Clade and within Araneoidea. The RTA Clade is a

263    large lineage of mostly cursorial spiders that includes such well-known groups as jumping and

264    wolf spiders (Salticidae and Lycosidae, respectively). The most recent common ancestor of the

265    RTA Clade has been traditionally understood as lacking foraging webs given the vast majority of

266    extant members of the clade do not have them. Types of webs traditionally used in phylogenetic

267    analyses (that is, variation in web architecture treated as states of a character) may not make

268    distinctions where superficial similarity masks important differences (e.g., brushed sheet-webs

269    and others discussed by Eberhard and Hazzi, 2017). The confluence of different methods of

270    ancestral character reconstruction, different web coding methods, different taxon samples and

271    tree topologies, and indeed disagreement on whether webs are a character at all has led to

272    misinterpretations and conflicting hypotheses on the evolution of webs.

273

274    Our analyses suggest that webs are ancestral for Araneae (see also Huang et al., 2018; Wang et

275    al., 2018), were subsequently lost in several lineages and only in a few instances in the RTA

276    Clade have evolved *de novo* in clades with cursorial ancestors. Orb webs also have a complex

277    evolutionary history. Our results are consistent with those from Fernández et al. (2018a, 2018b)

278    and Wolff et al. (2019) but not with those of Coddington et al. (2019). The latter found an

279    ancestral orb web probable in the common ancestor of Entelegynae, then secondarily lost in

280    numerous lineages. Coddington et al. (2019) also scored web presence and web architecture as

281    two different characters and "?" was used to score web type in the web architecture character

282    when the web was absent (i.e., treated as 'inapplicable'), but then they did not use SMMs and

283    reconstructed ancestral states for each of these characters independently. The two reconstructions

284    were displayed against each other and visually interpreted together. Their approach, however,

285    does not jointly estimate the marginal likelihood for both characters at internal nodes (although

286    they show a hierarchical relationship, as discussed above). In addition, scoring taxa where web is

287    absent is equivalent to polymorphic coding which implies that taxa with such scores are

288    interpreted as having some web architecture while they do not build foraging webs at all ("?"

289    notation is also used in the SMM approach of Tarasov (2019) but there it is handled specifically

290    as a result of the character amalgamation). These critical shortcomings indicate that the method

291    of Coddington et al. (2019) does not allow for proper treatment of hierarchically nested

292    characters and thus we did not use it here.

293

294    Our results suggest that the orb web evolved twice in the UDOH Grade and one (in the analyses

295    of the 13-state web architecture dataset) or up to three times (in the analyses of the two-state web

296    architecture data) in Araneoidea. In all cases, there are examples of subsequent losses that are

297    more granular than the scope of this work allows. In the latter, two of these events involved

298    subsequent losses. Within Araneidae, multiple lineages have much reduced or absent capture

299    webs, such as the genera *Chorizopes* and *Kaira*, while others have modified it beyond

300    recognition, such as the bolas spiders (mastophorine araneids). The other more complicated case

301    involves the tetragnathoid lineages, Mysmenidae, and Malkaridae. Most phylogenetic analyses

302    of tetragnathoids indicate Arkyidae as sister lineage to Tetragnathidae, and Mimetidae as sister

303    lineage to both. Arkyidae and Mimetidae both lack foraging  webs (Framenau et al., 2010;

304    Benavides et al., 2017), as do some lineages within Tetragnathidae (Gillespie, 1991) and all

305    Malkaridae (Hormiga and Scharff, 2020). The topology of the closely related lineages

306    Mysmenidae and Malkaridae are key to interpreting web evolution as well, given the former has

307    orb webs and the latter has none. Previous analyses (e.g., some but not all found by Fernández et

308    al. 2018a, 2018b) suggest a possible origin in the common ancestor of these five families, loss of

309    the orb web, and a new origin in Tetragnathidae. Here, we find a single origin of the orb webs of

310    tetragnathids and mysmenids, and three independent losses of the orb web in Arkyidae,

311    Mimetidae, and Malkaridae (Fig. 5).

312

313    Finally, it is interesting to note the differences in the inference of the number of origins of orb

314    webs in Araneoidea when web architecture is scored in two versus 13 states. Lumping character

315    states is expected to produce the same results if the scoring scheme with a higher number of

316    states is adequately partitioning the observed phenotypic variability (e.g., Tarasov, 2019). Thus,

317    our results support the idea expressed by us and others (see above) that we should continue to

318    work on improving our understanding of web architecture and its variability.

319

320    *Conclusions*

321

322    More loci and more taxa have allowed us to considerably improve our understanding of the

323    spider tree of life, corroborating established theories and sometimes proposing new relationships.

324    Our analyses placed many lineages in a genomic-scale phylogenetic framework for the first time

325    and continue to refute the single origin of orb webs within Araneae. The greater sophistication of

326    phylogenetic and comparative methods is not without caveats. Historically robust node support

327    measures seem to mask pervasively noisy signal, and coding and analytical variations in complex

328    trait reconstructions can generate disparate outcomes. Nonetheless, we believe this work

329    provides the foundation for the next steps in spider evolutionary studies.

330

331    FUNDING

340

353

354

355 REFERENCES

356

357 Álvarez-Padilla, F., Kallal, R. J., Hormiga, G. 2020. Taxonomy and phylogenetics of

358 Nanometinae and other Australasian orb-weaving spiders (Araneae: Tetragnathidae). Bull. Am.

359 Mus. Nat. Hist. 438, 1–107.

360

361 Ané, C., Larget, B., Baum, D. A., Dewitt Smith, S., Rokas, A. 2007. Bayesian estimation of

362 concordance among gene trees. Mol. Biol. Evol. 24, 412–426. doi: 10.1093/molbev/msl170

363

364 Ballesteros, J. A., Hormiga, G. 2016. A new orthology assessment method for phylogenomic

365 data: Unrooted Phylogenetic Orthology. Mol. Biol. Evol. 33, 2117–2134. doi:

366 10.1093/molbev/msw069

367

368 Beaulieu, J. M., Oliver, J. C., O'Meara, B. 2017. corHMM: Analysis of Binary Character

369 Evolution. R package version 1.22. https://CRAN.R-project.org/package=corHMM

370

371 Benavides, L. R., Giribet, G., Hormiga, G. 2017. Molecular phylogenetic analysis of "pirate

372 spiders" (Araneae, Mimetidae) with the description of a new African genus and the first report of

373 maternal care in the family. Cladistics 33, 375–405. doi: 10.1111/cla.12174

374

375 Blackledge, T. A., Scharff, N., Coddington, J. A., Szüts, T., Wenzel, J. W., Hayashi, C. Y.,

376 Agnarsson, I. 2009. Reconstructing web evolution and spider diversification in the molecular era.

377 Proc. Natl. Acad. Sci. USA. 106, 5529–5234. doi: 10.1073/pnas.0901377106

378

379     Bond, J. E., Garrison, N. L., Hamilton, C. A., Godwin, R. L., Hedin, M., Agnarsson, I. 2014.

380     Phylogenomics resolves a spider backbone phylogeny and rejects a prevailing paradigm for orb

381     web evolution. Curr. Biol. 24, 1765–1771. doi: 10.1016/j.cub.2014.06.034

382

383     Bott, R. A., Baumgartner, W., Bräunig, P., Menzel, F., Joel, A.-C. 2017. Adhesion enhancement

384     of cribellate capture threads by epicuticular waxes of the insect prey sheds new light on spider

385     web evolution. Proc. R. Soc. B 284, 20170363. doi: 10.1098/rspb.2017.0363

386

387     Brewer, M. S., Carter, R. A., Croucher, P. J., Gillespie, R. G. 2015. Shifting habitats,

388     morphology, and selective pressures: developmental polyphenism in an adaptive radiation of

389     Hawaiian spiders. Evolution 69, 162–178. doi: 10.1111/evo.12563.

390

391     Capella-Gutiérrez, S., Silla-Martínez, J. M, Gabaldón, T. 2009. trimAl: a tool for automated

392     alignment trimming in large-scale phylogenetic analyses. Bioinformatics 25, 1972–1973. doi:

393     10.1093/bioinformatics/btp348.

394

395     Cheng, D.-Q., Piel, H. W. 2018. The origins of the Psechridae: web-building lycosoid spiders.

396     Mol. Phylogenet. Evol. 125, 213–219. doi: 10.1016/j.ympev.2018.03.035

397

398     Coddington, J. A., Agnarsson, I., Hamilton, C. A., Bond, J. E. 2019. Spiders did not repeatedly

399     gain, but repeatedly lost, foraging webs. PeerJ 7, e6703. doi: 10.7717/peerj.6703

400

401     Dimitrov, D., Lopardo, L., Giribet, G., Arnedo, M. A., Álvarez-Padilla, F., Hormiga, G. 2012.

402     Tangled in a sparse spider web: single origin of orb weavers and their spinning work unravelled

403     by denser taxonomic sampling. Proc. R. Soc. B 279, 1341–1350. doi: 10.1098/rspb.2011.2011.

404

405     Dimitrov, D., Benavides, L. R., Arnedo, M. A., Giribet, G., Griswold, C. E., Scharff, N.,

406     Hormiga, G. 2017. Rounding up the usual suspects: a standard target-gene approach for

407     resolving the interfamilial relationships of ecribellate orb-weaving spiders with a new family-

408     rank. Cladistics 33, 221–250. doi: 10.1111/cla.12165.

409

410     Eberhard, W. G. 2018. Modular patterns in behavioural evolution: webs derived from orbs.

411     Behaviour 155, 1–35. doi: 10.1163/1568539X-00003502

412

413     Eberhard, W. G., Hazzi, N. A. 2017. Web building and prey wrapping behavior of *Aglaoctenus*

414     *castaneus* (Araneae: Lycosidae: Sosippinae). J. Arachnol. 45, 177–197. doi: 10.1636/JoA-S-16-

415     019.1

416

417     Eberle, J., Dimitrov, D., Valdez-Mondragón, A., Huber, B. A. 2018. Microhabitat change drives

418     diversification in pholcid spiders. BMC Evol. Biol. 18, 1–13. doi: 10.1186/s12862-018-1244-8

419

420     Enright, A. J., van Dongen, S., Ouzounis, C. A. 2002. An efficient algorithm for large-scale

421     detection of protein families. Nucleic Acids Res. 30, 1575–1584.

422

423     Faircloth, B. C. 2016. PHYLUCE is a software package for the analysis of conserved genomic

424     loci. Bioinformatics 32, 786–788.

425

426      Fernández, R., Hormiga, G., Giribet, G. 2014. Phylogenomic analysis of spiders reveals

427      nonmonophyly of orb weavers. Curr. Biol. 24, 1772–1777. doi: 10.1016/j.cub.2014.06.03

428

429      Fernández, R., Kallal, R. J., Dimitrov, D., Ballesteros, J. A., Arnedo, M. A., Giribet, G.,

430      Hormiga, G. 2018a. Phylogenomics, diversification dynamics, and comparative transcriptomics

431      across the Spider Tree of Life. Curr. Biol. 28, 1489–1497. doi: 10.1016/j.cub.2018.03.064.

432

433      Fernández, R., Kallal R. J., Dimitrov, D., Ballesteros, J. A., Arnedo, M. A., Giribet, G., Hormiga,

434      G. 2018b. Phylogenomics, diversification dynamics, and comparative transcriptomics across the

435      Spider Tree of Life (Correction). Curr. Biol. 28, 2190–2193. doi: 10.1016/j.cub.2018.06.018

436

437      Framenau, V. W., Scharff, N., Harvey, M. S. 2010. Systematics of the Australian orb-weaving

438      spider genus *Demadiana* with comments on the generic classification of the Arkyinae (Araneae:

439      Araneidae). Invertebr. Syst. 24, 139–171. doi: 10.1071/IS10005

440

441      French, A. S., Li, A. W., Meisner, S., Torkkel, P. H. 2014. Upstream open reading frames and

442      Kozak regions of assembled transcriptome sequences from the spider *Cupiennius salei*. Selection

443      or chance? Gene 539, 203–208. doi: 10.1016/j.gene.2014.01.079.

444

445      Gadagkar, S. R., Rosenberg, M. S., Kumar, S. 2005. Inferring species phylogenies from multiple

446      genes: Concatenated sequence tree versus consensus gene tree. J. Exp. Zool. Part B 304b, 64–74.

447

448 Garrison, N. L., Rodriguez, J., Agnarsson, I., Coddington, J. A., Griswold, C. E., Hamilton, C.

449 A., Hedin, M., Kocot, K. M., Ledford, J. M., Bond, J. E. 2016. Spider phylogenomics:

450 untangling the Spider Tree of Life. PeerJ. 4, e1719. doi: 10.1016/j.cub.2018.03.064

451

452 Gillespie, R. G. 1991. Hawaiian spiders of the genus Tetragnatha: I. Spiny leg clade J Arachnol.

453 19, 174–209

454

455 Griswold, C., Coddington, J., Hormiga, G., Scharff, N. 1998. Phylogeny of the orb-web building

456 spiders (Araneae, Orbiculariae: Deinopoidea, Araneoidea). Zool. J. Linn. Soc. Lond. 123, 1–99.

457

458 Guindon, S., Dufayard, J.-F., Lefort, V., Anisimova, M., Hordijk, W., Gascuel, O. 2010. New

459 algorithms and methods to estimate maximum-likelihood phylogenies: assessing the

460 performance of PhyML 3.0. Syst. Biol. 59, 307–321. doi: 10.1093/sysbio/syq010.

461

462 Hedin, M. 2015. High-stakes species delimitation in eyeless cave spiders (*Cicurina*, Dictynidae,

463 Araneae) from central Texas. Mol. Ecol. 24, 346–361. doi: 10.1111/mec.13036

464

465 Hedin, M., Derkarabetian, S., Ramírez, M. J., Vink, C., Bond, J. E. 2018. Phylogenomic

466 reclassification of the world's most venomous spiders (Mygalomorphae, Atracinae), with

467 implications for venom evolution. Sci. Rep. 8, 1636. doi: 10.1038/s41598-018-19946-2

468

469    Hedin, M., Derkarabetian, S., Alfaro, A., Ramírez, M. J., Bond, J. E. 2019. Phylogenomic

470    analysis and revised classification of atypoid mygalomorph spiders (Araneae, Mygalomorphae),

471    with notes on arachnid ultraconserved element loci. PeerJ 7, e6864. doi: 10.7717/peerj.6864

472

473    Hoang, D. T., Chernomor, O., von Haeseler, A., Minh, B.-Q., Vinh, L. S. 2018a. UFBoot2:

474    Improving the ultrafast bootstrap approximation. Mol. Biol. Evol. 35, 518–522. doi:

475    10.1093/molbe v/msx281

476

477    Hoang, D. T., Vinh, L. S., Flouri, T., Stamatakis, A., von Haeseler, A., Minh, B. Q. 2018b.

478    MPBoot: fast phylogenetic maximum parsimony tree inference and bootstrap approximation.

479    BMC Evol. Biol. 18, 11. doi: 10.1186/s12862-018-1131-3

480
481    Hormiga, G., Griswold, C. E. 2014. Systematics, phylogeny, and evolution of orb-weaving

482    spiders. Annu. Rev. Entomol. 59, 487–512. doi: 10.1146/annurev-ento-011613-162046

483

484    Hormiga, G., Scharff, N. 2020. The malkarid spiders of New Zealand (Araneae, Malkaridae).

485    Invertebr. Syst.s 34, 345–405. https://doi.org/10.1071/IS19073

486

487    Huang, D., Hormiga, G., Cai, C., Su, Yi., Yin, Z., Xia, F., Giribet, G. 2018. Origin of spiders and

488    their spinning organs illuminated by mid-Cretaceous amber fossils. Nat. Ecol. Evol. 2, 623–627.

489    doi: doi.org/10.1038/s41559-018-0475-9

490

491    Kalyaanamoorthy, S., Minh, B.-Q., Wong, T. K. F., von Haeseler, A., Jermiin, L. S. 2017.

492    ModelFinder: Fast model selection for accurate phylogenetic estimates. Nat. Methods 14, 587–

493    589. doi: 10.1038/Nmeth.4285

494

495    Kallal, R. J., Fernández, R., Giribet, G., Hormiga, G. 2018. A phylotranscriptomic backbone of

496    the orb-weaving spider family Araneidae (Arachnida, Araneae) supported by multiple

497    methodological approaches. Mol. Phylogenet. Evol. 126, 129–140. doi:

498    10.1016/j.ympev.2018.04.007.

499

500    Katoh, K., Standley, D. M. 2013. MAFFT multiple sequence alignment software version 7:

501    Improvements in performance and usability. Mol. Biol. Evol. 30, 772–780. doi:

502    10.1093/molbev/mst010

503

504    Kulkarni, S. S., Wood, H. M., Lloyd, M., Hormiga, G. 2019. Spider-specific probe set for

505    ultraconserved elements offers new perspectives on the evolutionary history of spiders

506    (Arachnida, Araneae). Mol. Ecol. Res. 20, 185-203. doi: 10.1111/1755-0998.13099

507

508    Kumar, S., Filipski, A. J., Battistuzzi, F. U., Kosakovksy Pond, S. L., Tamura, K. 2012. Statistics

509    and truth in phylogenomics. Mol. Biol. Evol. 29, 457–472. doi: 10.1093/molbev/msr202.

510

511    Kuntner, M., Hamilton, C. A., Cheng, R.-C., Gregorič, M., Lupse, N., Lokovsek, T., Lemmon, E.

512    M., Lemmon, A. R., Agnarsson, I., Coddington, J. A., Bond, J. E. 2019. Golden orbweavers

513   ignore biological rules: phylogenomic and comparative analyses unravel a complex evolution of

514   sexual size dimorphism. Syst. Biol. 68, 555–572. doi: 10.1093/sysbio/syy082.

515

516   Laumer, C. E, Fernández, R., Lemer, S., Combosch, D., Kocot, K. M., Riesgo, A., Andrade, S.

517   C. S., Sterrer, W., Sørensen, M. V., Giribet, G. 2019. Revisiting metazoan phylogeny with

518   genomic sampling of all phyla. Proc. R. Soc. B 286, 20190831. doi: 10.1098/rspb.2019.0831

519

520   Lopardo, L., Giribet, G., Hormiga, G. 2010. Morphology to the rescue: molecular data and the

521   signal of morphological characters in combined phylogenetic analyses—

522   a case study from mysmenid spiders (Araneae, Mysmenidae), with comments on the evolution of

523   web architecture. Cladistics 26, 1–52. doi: 10.1111/j.1096-0031.2010.00332.x

524

525   Magalhães, I. L. F., Azevedo, G. H. F., Michalik, P., Ramírez, M. J. 2020. The fossil record of

526   spiders revisited: implications for calibrating trees and evidence for a major faunal turnover since

527   the Mesozoic. Biol. Rev. 95, 184–217. doi:10.1111/brv.12559

528

529   Meng, X., Zhang, Y., Bao, H., Liu, Z. 2015. Sequence analysis of insecticide action and

530   detoxification-related genes in the insect pest natural enemy *Pardosa pseudoannulata*. PLoS One

531   10, e0125242. doi:10.1371/journal.pone.0125242

532

533   Michalik, P., Kallal, R. J., Dederichs, T. M., Labarque, F. M., Hormiga, G., Giribet, G., Ramírez,

534   M. J. 2019. Phylogenomics and genital morphology of cave raptor spiders (Araneae,

535    Trogloraptoridae) reveal an independent origin of a flow-through genital system. J. Zool. Syst.

536    Evol. Res. 57, 737–747. doi: 10.1111/jzs.12315

537

538    Minh, B. Q., Hanh, M. W., Lanfear, R. 2020. New methods to calculate concordance factors for

539    phylogenomic datasets.. Mol. Biol. Evol. doi:10.1093/molbev/msaa106

540

541    Mirarab, S., Reaz, R., Bayzid, M. S., Zimmermann, T., Swenson, M. S., Warnow, T. 2014.

542    ASTRAL: Genome-scale coalescent-based species tree estimation. Bioinformatics 30, 1541–

543    1548. doi: 10.1093/bioinformatics/btu462

544

545    Nguyen, L. T., Schmidt, H. A., von Haeseler, A., Minh, B.-Q. 2015. IQTREE: a fast and

546    effective stochastic algorithm for estimating maximum-likelihood phylogenies. Mol. Biol. Evol.

547    32, 268–274. doi: 10.1093/molbe v/msu300

548

549    Opatova, V., Hamilton, C. A., Hedin, M., Montes de Oca, L., Král, J., Bond, J. E. in press.

550    Phylogenetic systematics and evolution of the spider infraorder Mygalomorphae using genomic

551    scale data. Syst. Biol. doi: 10.1093/sysbio/syz064

552

553    Opell, B,D. 2013. Cribellar thread. In *Spider Ecophysiology*, ed. W. Nentwig, pp. 303–18.

554    Berlin/Heidelberg: Springer.

555

556    Paradis, E., Schliep, K. 2019. ape 5.0: an environment for modern phylogenetics and

557    evolutionary analyses in R. Bioinformatics 35, 526–528. doi: 10.1093/bioinformatics/bty633

558

559     Philippe, H., de Vienne, D. M., Ranwez, V., Roure, B., Baurain, D., Delsuc, F. 2017. Pitfalls in

560     supermatrix phylogenomics. Eur. J. Taxon. 283, 1–25. doi: 10.5852/ejt.2017.283

561

562     Piacentini, L. N., Ramírez, M. J. 2019. Hunting the wolf: a molecular phylogeny of the wolf

563     spiders (Araneae, Lycosidae). Mol. Phylogenet. Evol. 136, 227–240. doi:

564     10.1016/j.ympev.2019.04.004

565

566     R Core Team. 2019. R: A language and environment for statistical computing. R Foundation for

567     Statistical Computing, Vienna, Austria. URL https://www.R-project.org/.

568

569     Ramírez, M. J., Grismado, C. J., Ubick, D., Ovtcharenko, V. I., Cushing, P. E., Platnick, N. I.,

570     Wheeler, W. C., Prendini, L., Crowley, L. M., Horner, N. V. 2019. Myrmecicultoridae, a new

571     family of myrmecophilic spiders from the Chihuahuan Desert (Araneae, Entelegynae). Am. Mus.

572     Novit. 3930, 1–24. doi: 10.1206/3930.1

573

574     Rix, M. G., Cooper, S. J. B., Meusemann, K., Klopfstein, S., Harrison, S. E., Harvey, M. S.,

575     Austin, A. D. 2017. Post-Eocene climate change across continental Australia and the

576     diversification of Australasian spiny trapdoor spiders (Idiopidae: Arbanitinae). Mol. Phylogenet.

577     Evol. 109, 302–320. doi: 10.1016/j.ympev.2017.01.008

578

579     Robinson, D. F., Foulds, L. R. 1981. Comparison of phylogenetic trees. Math. Biosci. 53, 131–

580     147. doi: 10.1016/0025-5564(81)90043-2

581

582    Sanggaard, K. W., Bechsgaard, J. S., Fang, X., Duan, J., Dyrlund, T. F., Gupta, V., Jiang, X.,

583    Cheng, L., Fan, D., Feng, Y., Han, L., Huang, Z., Wu, Z., Liao, L., Settepani, V., Thøgersen, I.

584    B., Vanthournout, B., Wang, T., Zhu, Y., Funch, P., Enghild, J. J., Schauser, L., Andersen, S. U.,

585    Villesen, P., Schierup, M. H., Bilde, T., Wang, J. 2014. Spider genomes provide insight into

586    composition and evolution of venom and silk. Nat. Comm. 5, 3765. doi: 10.1038/ncomms4765

587

588    Sayyari, E., Mirarab, S. 2016. Fast coalescent-based computation of local branch support from

589    quartet frequencies. Mol. Biol. Evol. 33, 1654–1668. doi: 10.1093/molbev/msw079

590

591    Scharff. N., Coddington. J. A., Blackledge, T. A., Agnarsson, I., Framenau, V., Szüts, T.,

592    Hayashi, C. Y., Dimitrov, D. (2020). Phylogeny of the orb-weaving spider family Araneidae

593    (Araneae, Araneoidea). Cladistics 36, 1–21. doi: 10.1111/cla.12382

594

595    Shao, L., Li, S. 2018. Early Cretaceous greenhouse pumped higher taxa diversification in

596    spiders. Mol. Phylogenet. Evol. 127, 146–155. doi: 10.1016/j.ympev.2018.05.026

597

598    Sharma, P. P., Kaluziak, S. T., Pérez-Porro, A. R., González, V. L., Hormiga, G., Wheeler, W.

599    C., Giribet, G. 2014. Phylogenomic interrogation of arachnida reveals systemic conflicts in

600    phylogenetic signal. Mol. Biol. Evol. 31, 2963–2984. doi: 10.1093/molbev/msu235

601

602    Shear, W. A. 1986. Spiders: webs, behavior, and evolution. Stanford, California, USA: Stanford

603    University Press.

604

605    Simão, F. A., Waterhouse, R. M., Ioannidis, P., Kriventseva, E. V., Zdobnov, E. M. 2015.

606    BUSCO: assessing genome assembly and annotation completeness with single-copy orthologs.

607    Bioinformatics 31, 3210–3212. doi: 10.1093/bioinformatics/btv351

608

609    Smith, S. A., O'Meara, B. C. 2012. treePL: divergence time estimation using penalized

610    likelihood for large phylogenies. Bioinformatics 28, 2689–2690. doi:

611    10.1093/Bioinformatics/Bts492

612

613    Song, L., Florea, L. 2015. Rcorrector: efficient and accurate error correction for Illumina RNA-

614    seq reads. GigaScience 4, 48. doi: 10.1186/s13742-015-0089-y

615

616    Susko, E., Roger, A. J. 2020. On the use of information criteria for model selection in

617    phylogenetics.  Mol. Biol. Evol. 37, 549–562. doi: 10.1093/molbev/msz228

618

619    Tamura, K., Battistuzzi, F. U., Billing-Ross, P., Murillo, O., Filipski, A., Kumar, S. 2012.

620    Estimating divergence times in large molecular phylogenies. Proc. Natl. Acad. Sci. USA 109,

621    19333–19338. doi: 10.1073/pnas.1213199109

622

623    Tan, G., Muffato, M., Ledergerber, C., Herrero, J., Goldman, N., Gil, M., Dessimoz, C. 2015.

624    Current methods for automated filtering of multiple sequence alignments frequently worsen

625    single-gene phylogenetic inference. Syst. Biol. 64, 778–791. doi: 10.1093/sysbio/syv033

626

627    Tarasov, S. 2019. Integration of anatomy ontologies and evo-devo using structured Markov

628    models suggests a new framework for modeling discrete phenotypic traits. Syst. Biol. 68, 698–

629    716. doi: 10.1093/sysbio/syz005

630

631    van Dongen, S. 2000. Graphs clustering by flow simulation. Ph.D. thesis. University of Utrecht,

632    Utrecht.

633

634    Wang, B., Dunlop, J. A., Selden, P. A., Garwood, R. J., Shear, W. A., Müller, P., Lei, X. 2018.

635    Cretaceous arachnid *Chimerarachne yingi* gen. et. sp. nov. illuminates spider origins. Nat. Ecol.

636    Evol. 2, 614–622. doi: 10.1038/s41559-017-0449-3

637

638    Wheeler, W. C., Coddington, J. A., Crowley, L. M., Dimitrov, D., Goloboff, P. A., Griswold, C.

639    E., Hormiga, G., Prendini, L., Ramírez, M. J., Sierwald, P., Almeida-Silva, L., Álvarez-Padilla,

640    F., Arnedo, M. A., Benavides Silva, L. R., Benjamin, S. P., Bond, J. E., Grismado, C. J., Hasan,

641    E., Hedin, M., Izquierdo, M. A., Labarque, F. M., Ledford, J., Lopardo, L., Maddison, W. P.,

642    Miller, J. A., Piacentini, L. N., Platnick, N. I., Polotow, D., Silva-Dávila, D., Scharff, N., Szüts,

643    T., Ubick, D., Vink, C. J., Wood, H. M., Zhang, J. X. 2017. The spider tree of life: phylogeny of

644    Araneae based on target-gene analyses from an extensive taxon sampling. Cladistics 33, 574–

645    616. doi: 0.1111/cla.12182.

646

647    Wolff, J. O., Paterno, G. B., Liprandi, D.,  Ramírez, M. J., Bosia, F., van der Meijden, A.,

648    Michalik, P., Smith, H. M., Jones. B. R., Ravelo, A. M., Pugno, N., Herberstein, M. E. 2019.

649 Evolution of aerial spider webs coincided with repeated structural optimization of silk

650 anchorages. Evolution 73, 2122–2134. doi: 10.1111/evo.13834

651

652 Wood, H. M., González, V. L., Lloyd, M., Coddington, J. A., Scharff, N. 2018. Next-generation

653 museum genomics: phylogenetic relationships among palpimanoid spiders using sequence

654 capture techniques (Araneae: Palpimanoidea). Mol. Phylogenet. Evol. 127, 907–918. doi:

655 10.1016/j.ympev.2018.06.038.

656

657 Wood, H. M., Griswold, C. E., Gillespie, R. G. 2012. Phylogenetic placement of pelican spiders

658 (Archaeidae, Araneae), with insight into the evolution of the "neck" and predatory behaviours of

659 the superfamily Palpimanoidea. Cladistics 28, 598–626. doi: 10.1111/j.1096-0031.2012.00411.x

660

661 World Spider Catalog. 2020. World Spider Catalog. Version 20.5. Natural History Museum

662 Bern. Available from: URL http://wsc.nmbe.ch (accessed on 8 January 2020). doi: 10.24436/2.

663

664 Yang, Z. 2007. PAML 4: phylogenetic analysis by maximum likelihood. Mol. Biol. Evol. 24,

665 1586–1591. doi: 10.1093/molbev/msm088.

666

667 Zhang, Z.-Q. 2011 Animal biodiversity: an introduction to higher-level classification and

668 taxonomic richness. Zootaxa 12, 7–12.

669

670    Zhao, Y. J., Zeng, Y., Chen, L., Dong, Y., Wang, W. 2014. Analysis of transcriptomes of three

671    orb-web spider species reveals gene profiles involved in silk and toxin. Insect Sci. 21, 687–698.

672    doi: 10.1111/1744-7917.12068.

673

674

675

676

677

678

679

680

681

682

683

684

685

686

687

688

689

690

691

692

693     **Figure 1.** A sample of the diversity of webs and foraging strategies in araneomorph spiders. (a),

694     *Deinopis* sp. (Deinopidae) from Madagascar, a cribellate weaver with a highly modified orb

695     web. (b), The ecribellate orb web of *Ocrepeira darlingtoni* (Araneidae), from the Dominican

696     Republic. (c), The modular vertical web of *Synotaxus* sp. (Synotaxidae), from Brazil. (d), A

697     typical web of Linyphiidae, from Taiwan. (e), The cribellate orb web of an uloborid from

698     Australia. (f), The ecribellate orb web of *Maxanapis* sp. (Anapidae), from Australia. (g),

699     *Exechocentrus lancearius* (Araneidae), a bolas spider from Madagascar. (h), The sheet web of

700     *Runga* sp. (Physoglenidae) from New Zealand. (i), A typical aerial sheet web of a cyatholipid

701     from Australia. (j), The characteristic tent web of *Oecobius* sp. (Oecobiidae), from Tobago. (k),

702     The cribellate web of *Paramatachia* sp. (Desidae), from Australia, a member of the RTA Clade.

703     (l), The highly modified orb web of a mysmenid from Madagascar. (m), The webless

704     plapimanoid spider *Eriauchenius workmani* (Archaeidae) feeding on a theridiid spider in

705     Madagascar (all photos by G. Hormiga).

706

707     **Figure 2**. Spider tree of life, non-araneoid and close relatives. Derived from BUSCO orthology,

708     67% occupancy, trimmed using trimAl, and maximum likelihood analysis using IQ-TREE. (a),

709     arachnid outgroup taxa, Mesothelae, Mygalomorphae, and non-entelegyne araneomorphs. (b)

710     UDOH Grade and RTA Clade. (c ) full tree highlighting regions (a) and (b).

711

712     **Figure 3.** Phylogenetic relationships of araneoids and close relatives. Derived from BUSCO

713     orthology, 67% occupancy, trimmed using trimAl, and maximum likelihood analysis using IQ-

714     TREE. (a) Eresidae, Nicodamoidea, and Araneoidea, derived from BUSCO orthology, 67%

715     occupancy, trimmed using trimAl, and maximum likelihood analysis using IQ-TREE. (b) full

716     tree highlighting eresids, nicodamoids, and araneoids. (c-e), Different topologies generated by

717     UPhO orthology, 33% occupancy, trimmed using trimAl, and maximum likelihood analysis

718     using IQ-TREE. (c ), Malkarid, mysmenid, and tetragnathoid clade. (d), Physoglenid, synotaxid,

719     and nesticid clade. (e), Araneid lineage except Phonognathinae and Nephilinae.

720

721     **Figure 4.** Calibrated phylogram using treePL, with major groups highlighted. Stars represent

722     fossil placements. Stars inside collapsed clades represent at least one calibration point within that

723     clade.

724

725     **Figure 5.** Ancestral state reconstruction of foraging webs and their architecture using the

726     structured Markov models. The results shown here are based on the 13 states scoring scheme for

727     the web architecture and a 2-rates model which resulted in the best BIC score. Differences with

728     reconstructions based on 2 states scoring scheme for web architecture are shown in the top right

729     left corner (based on the best scoring model – a 2-rates model with one hidden state for the orb

730     web state; only the Araneoidea clade is depicted here). Full versions of these results with tip

731     labels are provided as supplementary materials on Harvard Dataverse.

732

733     **Table 1.** Matrix construction and analyses. Where the number of sites is presented as a single

734     value, it is the trimmed matrix; two values signify trimmed and untrimmed version of the matrix.

735

736     **Table 2**. Selected clades relevant to Araneoidea and their support values. Analytical

737     abbreviations: Method B, BUSCO orthology on the *all* dataset with 67% occupancy; Method U,

738     UPhO orthology on the *ara* dataset with 33% occupancy; UFB (Tr/Un), ultrafast bootstrap

739    support on trimmed and untrimmed matrices; SH-aLRT, Shimodaira-Hasegawa approximate

740    likelihood ratio test; gCF, gene concordance factor; sCF, site concordance factor; LPP (Tr/Un),

741    local posterior probability on trimmed or untrimmed matrix. In the latter, where the ASTRAL

742    topology differs from that of the maximum likelihood topology, that alternative is given with its

743    supports. Taxon abbreviations: Ana, Anapidae; ARA, araneoids; Ara, Araneidae; Ere, Eresidae;

744    Mal, Malkaridae; Mys, Mysmenidae; Nes, Nesticidae; NIC, nicodamoids; Phy, Physoglenidae;

745    Sym, Symphytognathidae; Syn, Synotaxidae; Tet, tetragnathoids; The, Theridiosomatidae.